文章编号: 1001－2060(2005)05－0478－04

电加热倾斜管温度场分布计算

高　峰, 尹　飞, 陈听宽, 罗毓珊
(西安交通大学 动力工程多相流国家重点实验室, 陕西　西安　710049)

摘　要: 考虑自然对流对倾斜上升管内流体传热的影响, 将外壁温度与外壁热负荷作为边界条件, 同时将内热源作为并联网格电阻放热来进行处理, 为电加热倾斜管温度场分布建立二维数学模型。根据空间节点推进的控制容积差分法求解流体换热和管壁导热耦合决定的电加热倾斜管二维温度场导热反问题, 编制计算程序, 针对我国第一台超临界锅炉螺旋管圈水冷壁的管型进行了管壁温度场的计算。在亚临界及超临界压力工况下, 计算结果都可以很好地反映倾斜管壁温的分布规律, 同时计算收敛性良好。

关　键　词: 电站锅炉; 温度场; 源项; 倾斜管; 热负荷
中图分类号: TK124　　文献标识码: A

1　前　言

倾斜管内流体传热广泛存在于蒸汽发生器, 以及各种工业设备中。电站锅炉螺旋管圈水冷壁就采用倾斜上升的布置方式。现代大型超临界锅炉多采用螺旋管圈水冷壁的型式。为了满足我国电站超临界锅炉国产化的技术需求, 需要深入研究倾斜上升管内流体传热的特性。国内外对于管内流体传热的研究多采用电加热的方式, 直接在试验管壁上通以低电压、大电流的交流电, 凭借管子本身电阻产生热量来加热管内工质。本课题预热段与试验段均采用低电压、高电流的交流电直接对其加热, 电功率通过调压变压器连续调节, 加热总功率共 840 kW, 其中试验段为 180 kW, 其它为预热段管子加热功率。试验段外壁温度以及工质温度均由热电偶测得, 而试验段内壁温度、内壁热负荷均需要通过计算得到。

忽略了沿电加热倾斜管轴向的导热, 可以将电加热倾斜管温度场作为二维温度场来进行处理。倾斜上升管内壁面的边界条件既非定热流, 也非定壁温。它是由流体与管内壁换热和管壁导热耦合决定的二维温度场的导热反问题, 因此, 不能采用传统的处理导热正问题的方式来对其求解。对于此种问题, Taler、Yang、Hsu 和 Tseng 等人都进行了大量的研究工作[1~4], 先后提出了有限元、有限差分、适体坐标等求解方法。

本次西安交通大学动力工程多相流国家重点实验室对我国第一台国产超临界锅炉——华能沁北电厂 2× 600 MW 超临界直流锅炉水冷壁传热特性的研究就是采用电加热的方式来完成的。因此, 开发电加热倾斜管温度场分布计算程序, 对其管壁温度场分布进行求解计算是非常必要而且有意义的。

2　数学模型

本课题中, 对于电加热倾斜管二维温度场的求解是采用 Taler 所提出的空间节点推进的控制容积差分法[1]。空间节点推进的主要思想是将测得的外壁温度作为外壁面的边界条件, 通过传热量把外壁温度和内点联系起来。邻近外壁的第二层节点的温度可以根据外壁温度和外壁散热量来求得。同理, 第三层节点温度可以由第二层节点温度和传热量来求得。依此类推, 就可以得到内壁面节点的温度, 进而可以求得内壁热负荷。本文中流体与管内壁的换热系数采用文献[5] 的倾斜上升管换热系数关联式来确定。

2.1　控制方程

考虑沿重力方向的对称性, 所以将圆管截面的一半作为计算区域。图 1 表示倾斜管的计算区域。由以上分析可知, 在计算倾斜管温度场时, 需要采用有内热源的二维导热方程, 而有内热源的二维稳态温度场的导热偏微分方程在极坐标系中的形式如下:

收稿日期: 2005－03－07;　修订日期: 2005－04－26
基金项目: 国家自然科学基金资助项目(50323001)
作者简介: 高　峰(1963－), 男, 山东东明人, 西安交通大学高级工程师.

$$\frac{1}{r}\frac{\partial}{\partial r}\left[r\lambda\frac{\partial T}{\partial r}\right]+\frac{1}{r}\frac{\partial}{\partial\theta}\left[\frac{\lambda}{r}\frac{\partial T}{\partial\theta}\right]+S=0 \tag{1}$$

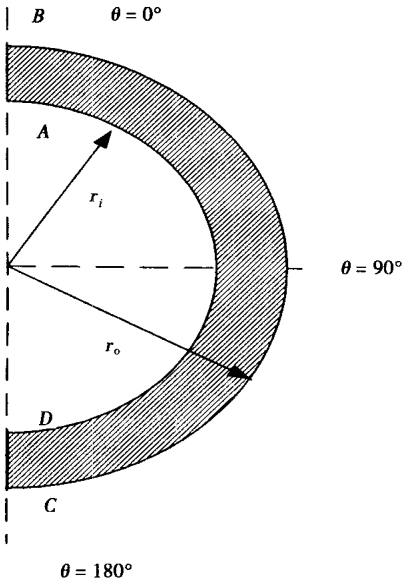

图 1　倾斜管计算区域

边界条件如下:

$$T=T_w \qquad (r_i=r_0) \tag{2}$$

$$q_w=0 \qquad (r_i=r_0) \tag{3}$$

其中电加热试验管在达到热平衡后的吸热效率可以采用下式求得:

$$\eta=\Delta H/Q_E \tag{4}$$

2.2　方程离散化

在得到控制方程和边界条件的基础上, 需要对计算区域进行离散化。在计算截面周向上划分 M 个节点, 径向上划分 N 个节点。外壁面为径向第一层节点, 内壁面为径向第 N 层节点。这样就将圆管划分为 $M\times N$ 个节点, 从而形成了 $(M-1)\times(N-1)$ 个控制容积。将式(1)在控制体 P(如图 2)内积分, 可以得到其离散形式为:

$$a_pT_p=a_ET_E+a_wT_w+a_NT_N+a_ST_S+b \tag{5}$$

其中:

$$a_E=\frac{\Delta r}{r_e(\delta\theta)_e/\lambda_e},\qquad a_w=\frac{\Delta r}{r_w(\delta\theta)_w/\lambda_w},$$
$$a_N=\frac{r_n\Delta\theta}{(\delta r)_n/\lambda_n},\qquad a_s=\frac{r_s\Delta\theta}{(\delta r)_s/\lambda_s} \tag{6}$$

$$a_p=a_E+a_w+a_N+a_S+a_P^0+S_p\Delta V \tag{7}$$

$$b=S_C\Delta V=S\Delta V=S(0.5(r_n+r_s)\Delta r\Delta\theta) \tag{8}$$

在本试验所处理的稳态问题中, $a_p^0=0$。同时, 式(1)中的源项 $S=S_C-S_pT_p$ 中的 $S_p=0$。则式(7)可写为:

$$a_p=a_E+a_W+a_N+a_s \tag{9}$$

将式(5)以节点的形式表示并整理得:

$$T(I,J+1)=(a_pT(I,J)-a_ET(I+1,J)+a_wT(I-1,J)-a_NT(I,J-1)-b)/a_s \tag{10}$$

从上式可知: 在第 J 和第 $J-1$ 层的节点温度已知的情况下, $J+1$ 层的节点温度可以从上式算出。这就是所谓得空间节点推进。

在外边界上, 已知的节点温度只有一层, 此时的求解就需用到外壁面的热负荷。

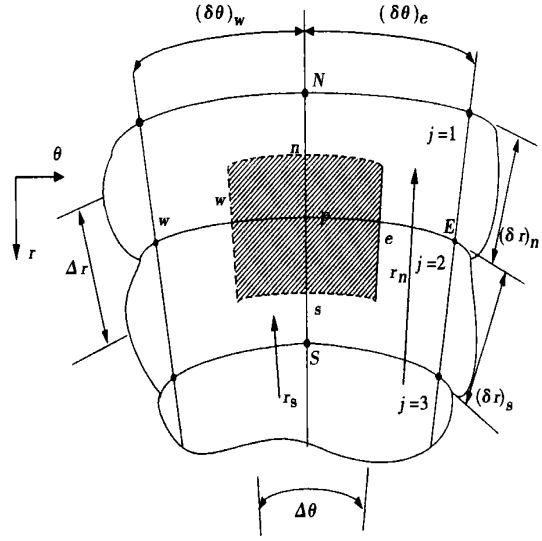

图 2　计算区域在极坐标中的网格形式

2.3　源项的处理

对于计算中的热源项可采用如下处理方法, 如果取轴线方向上的单位长度, 这样就相当于 $(M-1)\times(N-1)$ 个并联电阻在电压 U 下发热。因此, P 控制体的发热量为:

$$Q'=U^2/R(I,J) \tag{11}$$

其中单位长度控制体 P 的电阻:

$$R(I,J)=\rho(I,J)/F(I,J) \tag{12}$$

式中: $F(I,J)$—控制体截面积; $\rho(I,J)$—控制体电阻率。体积内热源为:

$$S=\frac{Q'}{\Delta V}=\frac{2Q'}{(r_n+r_s)\Delta r\Delta\theta} \tag{13}$$

2.4　温度场求解步骤

按照以上方法使控制方程离散化并得到边界条件之后, 温度场的求解步骤如下:

(1)先假定一个温度场的分布; (2)计算区域内各点上的导热系数和电阻率根据给定的温度场分布

得到，再根据以此确定的电阻率分布，进一步得到各控制容积的电阻大小；

(3)按照 TDMA(倾斜管)算法依次在全场迭代，求得新的温度分布；

(4)将算得的新温度场代替旧温度场，重复步骤(1)和(2)，直至相邻两次迭代的节点最大温度差小于 0.001 ℃，就可以认为迭代收敛，也即得到的温度场为真实温度场，此时的内壁温度为计算内壁温度。

2.5 内壁热流密度求解

采用以上方法算得计算区域温度场之后，就可以用第 N 层和 $N-1$ 层的温度来求得内壁局部热流密度，计算式如下：

$$q_i = 1/r_i \Delta\theta (a_S T(I, N-1) + a_E (I+1, N) + a_w (I-1, N) - a_p (I, N) + b) \quad (14)$$

在计算中，把试验圆管划分为 30 等份的网格，周向划分间隔为 30°，周向网格数为 12。

3 算例分析

按照以上算法，编制程序计算电加热倾斜管二维温度场分布，整理亚临界计算结果，做出压力 $p=19$ MPa、质量流速 $G=600$ kg/(m^{2}s)、热负荷 $q=400$ kW/m^2 时，倾斜管周向各点内壁温度随焓值的变化曲线如图 3 所示。本文中把倾斜管顶点记为 $\theta=0°$，按顺时针方向，将倾斜管底点记为 $\theta=180°$。由图可见，管壁顶点发生壁温飞升(通常指倾斜管的第一次壁温飞升)后，随着干度的增加，顶点的壁温逐渐增加到极大值，之后开始下降。但是随着管壁底点发生壁温飞升，顶点壁温又重新开始上升，即发生所谓的第二次壁温飞升，而且顶点的第一次壁温飞升峰值较大，第二次壁温飞升峰值相对较小。在顶点处发生传热恶化之后，底点处发生传热恶化之前，在相当大的焓值范围内存在着同一管截面上半部分为膜态沸腾，下半部分为核态沸腾的现象，而且顶点处的壁温总是最高。

图 4 表示压力 $p=19$ MPa、质量流速 $G=600$ kg/(m^{2}s)、热负荷 $q=400$ kW/m^2 时，内壁温度周向分布曲线。由图可见，壁温飞升总是首先在顶点处发生，随着干度的增加，传热恶化区的范围逐渐扩大。顶点处可以在较低干度，甚至在负干度条件下，发生壁温飞升。而底点处却总在干度很高时，才发生壁温飞升。当底点处发生传热恶化后，整个圆周壁温均开始飞升，而且管壁的周向壁温最大差值发生在管壁顶点与底点之间。

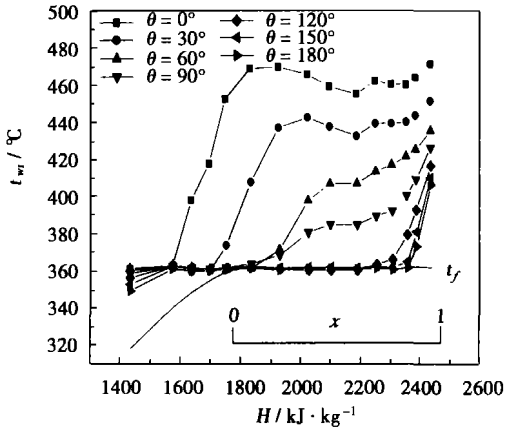

图 3 周向各点内壁温度随焓值的变化曲线

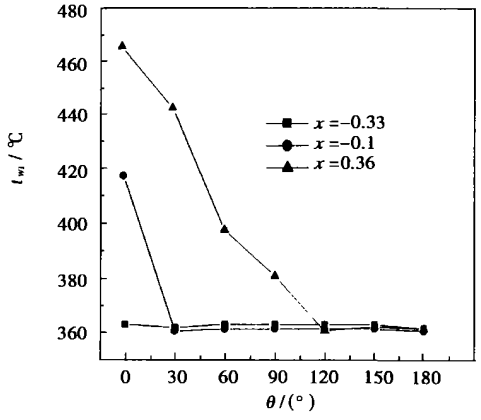

图 4 内壁温度周向分布曲线

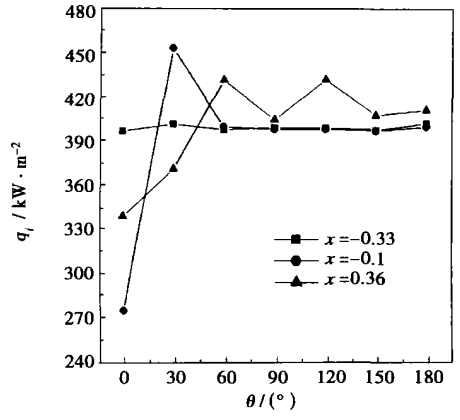

图 5 内壁热负荷周向分布曲线

图 5 表示压力 $p=19$ MPa、质量流速 $G=600$ kg/(m^{2}s)、热负荷 $q=400$ kW/m^2 时，内壁热负荷周向分

布曲线。由图可见, 在传热恶化发生前, 内壁热负荷沿周向均匀分布; 传热恶化发生后, 由于管壁导热作用, 造成热负荷重新分布。膜态沸腾的高温区内壁热负荷降低, 核态沸腾的低温区内壁热负荷不变, 膜态沸腾与核态沸腾区的交界处内壁热负荷增大。

整理超临界计算结果, 做出压力 $P=26$ MPa, 质量流速 $G=600$ kg/(m^2s), 热负荷 $q=250$ kW/m^2 及工质焓值 $H=2\ 072$ kJ/kg 时, 倾斜管内壁温度及内壁热负荷的周向分布曲线如图 6 所示。在超临界压力区, 汽液并存现象消失, 管内流体以单相形式存在。但是, 受重力作用, 较轻的热流体会向倾斜管顶点运动, 不断上升的热流体不但在倾斜管顶点形成一个上驻点, 而且会在倾斜管底点形成一个下驻点, 这样在管壁同一周向截面上会有上下两个驻点形成。下驻点很容易被冷流体所补充, 从而得到冷却, 因此管壁底点传热系数较高, 壁温较低; 而上驻点很可能形成流体的脱体流动, 管壁顶点传热系数降低, 顶点壁温升高。沿管壁周向, 从顶点到底点壁温降低, 这样会引起由倾斜管顶点到底点的周向导热, 从而产生了管壁均流作用, 以致倾斜管内壁顶点的热负荷略低于其底点的热负荷, 而且内壁热负荷沿管壁周向是变化的。但是对比亚临界数据可以发现, 超临界压力下倾斜管内壁温度以及内壁热负荷的周向不均匀差值要远低于亚临界压力下的相应值, 这说明超临界压力下倾斜管周向不均匀性较亚临界压力下要更为缓和。

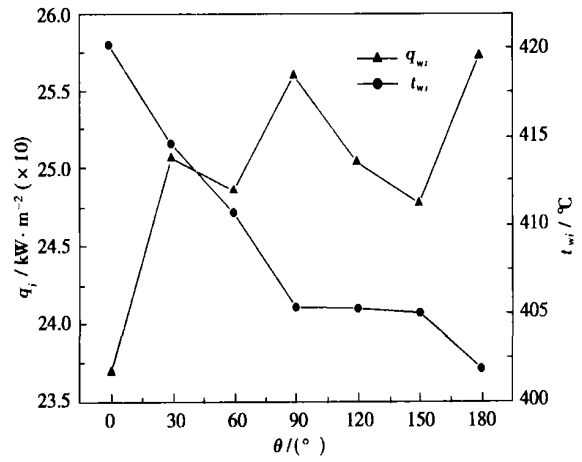

图 6　内壁温度及内壁热负荷周向分布曲线

4　结　论

(1)为电加热倾斜管温度场分布建立数学模型, 将内热源作为并联网格电阻放热来处理, 同时将外壁温度与外壁热负荷作为边界条件, 根据空间节点推进的控制容积差分法, 求解流体换热和管壁导热耦合决定的电加热倾斜管二维温度场的导热反问题, 编制计算程序, 计算求解电加热倾斜管二维温度场。

(2)根据亚临界压力区的计算结果, 倾斜上升管有两次壁温飞升, 倾斜管顶点首先发生壁温飞升, 随后沿周向各点壁温依次飞升, 当管壁底点发生壁温飞升后倾斜管整体壁温开始飞升。管壁的周向壁温最大差值发生在管壁顶点与底点之间。在超临界压力区, 倾斜管内壁形成上下两个驻点, 管壁温度从顶点到底点降低, 但是管壁温差相对亚临界压力区要小很多。与亚临界压力区类似, 超临界压力区倾斜管由于其管壁均流的作用, 顶点的热负荷略低于其底点的热负荷, 而且内壁热负荷沿管壁周向是变化的。

(3)计算结果所得规律符合倾斜管在亚临界以及超临界压力范围的温度场分布规律, 证明程序算法正确。

参考文献:

[1] TALER J, ZIMA W. Solution of inverse heat conduction problems using control volume approach[J]. **International Journal of Heat Mass Transfer**, 1999, **42**: 1123－1140.

[2] YANG Y T, HSU P T, CHEN C K. A three-dimensional inverse heat conduction problem approach for estimating the heat flux and surface temperature of a hollow cylinder[J]. **J of Physics D: Applied Physics**, 1997, **30**: 1326－1333.

[3] HSU P T, YANG Y T, CHEN C K. Simultaneously estimating the initial and boundary conditions in a two－dimensional hollow cylinder[J]. **Int J Heat Mass Transfer**, 1998, **41**: 219－227.

[4] TSENG A A, CHEN T C, ZHAO F Z. Direct sensitivity coefficient method for solving two-dimensional inverse heat conduction problem by finite－element scheme[J]. **Numerical Heat Transfer**, 1995, **27**: 291－307.

[5] 胡志宏. 超临界和近临界压力区垂直上升及倾斜管传热特性研究[D]. 西安: 西安交通大学, 2002.

不同冲角端壁翼刀控制压气机叶栅二次流的实验研究＝**An Experimental Investigation of the Control of Compressor Cascade Secondary Flows by the Use of Endwall Fences at Different Incidences** [刊, 汉] /TIAN Fu, ZHONG Jing-jun (The School of Energy Science and Engineering under the Harbin Institute of Technology, Harbin, China, Post Code: 150001), CHEN Ying (Harbin No. 703 Research Institute, Harbin, China, Post Code: 150036) //Journal of Engineering for Thermal Energy & Power. — 2005, 20(5). —464 ~468

An experimental investigation was conducted of a compressor cascade with endwall fences installed at different circumferential locations under different incidences. It has been found that the cascade total loss tends to be reduced when the endwall fences are far away from a suction surface and will tend to increase when the fences are near the suction surface. In case of a change in incidences the optimum fence location for achieving a decrease in cascade total loss will undergo a change. If the endwall fences are installed at a distance of 70% relative pitch from the suction- surface location, the cascade total loss within a certain range of incidences (-9° ~ +6°) will still be lower than that in conventional cascades. Under a negative incidence the impact of fence installation on an in-channel flow will tend to decrease with an increase in incidence. Under a positive incidence the impact of fence installation on an in-channel flow will tend to strengthen with an increase in incidence. **Key words**: compressor cascade, endwall fence, incidence, cascade loss

倒角和间隙对跨音轴流压气机气动性能的影响＝**The Influence of Blade Root Fillet and Blade Tip Clearance on the Aerodynamic Performance of a Transonic Axial Compressor** [刊, 汉] /MAO Ming-ming, SONG Yan-ping, WANG Zhong-qi (The School of Energy Science and Engineering under the Harbin Institute of Technology, Harbin, China, Post Code: 150001) //Journal of Engineering for Thermal Energy & Power. — 2005, 20(5). —469 ~473

Through the numerical simulation of the flow field of a single-stage transonic axial compressor a study was conducted of the impact of rotating-blade root fillet and tip clearance on the flow field aerodynamic performance. The results of the study indicate that the blade tip clearance will lead to a flow blockage at the top zone and increase the separation loss at that zone. The blade root fillet will decrease the flow turning angle at the blade root, decrease work-performing capacity and enlarge the blade root separation zone. This will lead to a decrease in flow rate and an increase in separation loss at the root zone. In view of the above, the rotating blade tip clearance and the blade root fillet should be taken into account in order to enhance the accuracy of the numerical simulation. **Key words**: transonic axial compressor, numerical simulation, blade tip clearance, blade root fillet

矩形管湍流冲击射流流动与传热的数值研究＝**Numerical Study of the Flow and Heat Transfer of a Rectangular-tube Turbulent Impinging Jet Flow** [刊, 汉] /CHEN Qing-guang, WU Yu-lin (Department of Thermal Energy Engineering, Tsinghua University, Beijing, China, Post Code: 100084), ZHANG Yong-jian, WANG Tao (Shandong University of Science & Technology, Qingdao, China, Post Code: 266510) //Journal of Engineering for Thermal Energy & Power. — 2005, 20(5). —474 ~477

By employing algorithm SIMPLE and a RNG $k-\varepsilon$ turbulent model and through the solution of a three-dimensional $N-S$ equation and energy equation a numerical simulation was performed of a rectangular-tube turbulent impinging jet flow with Reynolds number of 10000 and an impingement height of 4 times of nozzle hydraulic diameter. It has been found that at the jet flow cross-section near the impingement surface accompanied by the appearance of two counter-rotating vortex pairs there emerge two eccentric peak values of main stream velocity. An analysis shows that the formation of the dual-eccentric velocity peak values is caused by the vorticity upstream diffusion produced by the impingement surface. An investigation of the temperature field and the local Nusselt number distribution of the impingement surface indicates that heat transfer characteristics of the jet flow are controlled by the flow structure and the use of a rectangular-tube turbulent jet flow can result in a relatively large impingement zone and more uniform cooling effectiveness. **Key words**: rectangular-tube impingement jet, numerical simulation, eccentric peak value, heat transfer

电加热倾斜管温度场分布计算＝**Calculation of the Temperature Field Distribution in an Electrically Heated In-**

clined Tube [刊, 汉] /GAO Feng, YIN Fei, CHEN Ting-kuan, et al (National Key Laboratory of Multi-phase Flow in Power Engineering under the Xi' an Jiaotong University, Xi' an, China, Post Code: 710049) //Journal of Engineering for Thermal Energy &Power. — 2005, 20(5). —478 ~481

Taking into account the impact of natural convection on the fluid heat transfer in an inclined riser tube the outer wall temperature and heat load are assumed as boundary conditions. Meanwhile, with the internal heat source being treated as a parallel-connected network resistance heat-release a two-dimensional mathematical model was set up for assessing the temperature field distribution in an electrically heated inclined tube. A controlled-volume differential method based on spatial node advance was used to solve the inverse problem of a two-dimensional temperature field heat conduction in an electrically heated inclined tube, which is determined by the coupling of fluid heat exchange and tube wall heat conduction. A computation program was prepared and the calculation of tube-wall temperature field conducted for the tube type of the spiral tube-coil water-wall of the first supercritical-parameter boiler in China. Under the operating condition of subcritical and supercritical pressures the calculation results can all truly reflect the wall-temperature distribution law of the inclined tube with a fairly good computation convergence being attained. **Key words**: temperature field, source item, inclined tube, thermal load

辐射离散传播法在三维圆柱腔体辐射传热计算中的应用= **The Application of a Radiation Discrete Transfer Method for the Radiation Heat Transfer Calculation of a Three-dimensional Cylindrical Cavity Body** [刊, 汉] /GU Ming-yan, ZHANG Ming-chuan, FAN Wei-dong, et al (Mechanical &Power Engineering Institute under the Shanghai Jiaotong University, Shanghai, China, Post Code: 200240) //Journal of Engineering for Thermal Energy &Power. — 2005, 20(5). —482 ~485

By employing a method combining spatial analytical geometry theory with numerical calculations a radiation discrete transfer method (DTM) was implemented for the radiation heat transfer calculations in a three-dimensional cylindrical cavity body. Through the use of coordinate transformation a radiation ray equation was set up. By directly solving the intersection points of the radiation rays in various three-dimensional angles with various radiation unitary bodies at all emission points determined were the path traversed by the rays and the distance between the various intersecting points and emission points. Then, with the intersecting points being arranged in proper order, and taking into account the magnitude of the above-mentioned distance, one can obtain the intersecting point sequence for solving the radiation energy transfer equation in adaptation to the DTM method. The above-mentioned method was used to perform a three-dimensional calculation of the radiation heat exchange in the cylindrical cavity body and the computation results are in basic agreement with those of a precision solution. The DTM method was employed for calculating the radiation heat exchange in a pulverized-coal combustion flame. The temperature field being obtained basically agrees with that of experimental results and the surface radiation heat-flux density assumes a rational distribution. This shows that the method designed by the authors is feasible. **Key words**: radiation transfer equation, discrete transfer method, three-dimensional cylindrical cavity body

汽液相变系统的平衡稳定性分析= **Equilibrium Stability Analysis of a Liquid-vapor Phase Transition System** [刊, 汉] /WU Shuang-ying, ZENG Dan-ling, LI You-rong (Power Engineering College under the Chongqing University, Chongqing, China, Post Code: 400044) //Journal of Engineering for Thermal Energy &Power. 2005, 20(5). —486 ~488

On the basis of the theory of non-equilibrium thermodynamics and through the introduction of an important work/potential function in the heat exchange process of a liquid-vapor phase transition, the so-called available energy, an analysis was conducted of the available energy of the liquid-vapor phase transition system. As a result, a calculation formula for the available energy variation of the liquid-vapor phase transition system was obtained, and using this as criteria an analysis was performed of the stability of the liquid-vapor phase transition system. Thus, obtained were the phase equilibrium conditions of the above-mentioned system, mechanics stability conditions and thermal stability conditions with relevant physical meanings being also given. Furthermore, a definition is provided for the liquid and vapor phase force-stable marginal curves during the liquid-vapor phase transition. It can be shown that the force-stable condition of the liquid-vapor phase